Full Paper

Propellants, Explosives, Pyrotechnics

DOI: 10.1002/prep.202000195

Characterization of the Detonation Pressure of a PETN Based PBX with the Optical Active Method

Joana Quaresma,*[a, b] Lukas Deimling,[a] Jose Campos,[b] and Ricardo Mendes[b]

Abstract: Detonation metrology is essential for the development of energetic materials, to characterize existing explosives, and to characterize materials behavior under high pressures. The optical active method (OAM), based on PMMA optical fibers (250 μm diameter) and their radiation transmission loss when shocked, was used to characterize the detonation wave (DW) and shock wave (SW) in inert barriers and applied to measure the detonation pressure in condensed explosives. The detonation velocity and detonation pressure of a PBX based on PETN (86% PETN, 14% Sylgard), known as Seismoplast were measured. The OAM with protected optical probes (POP) was used to determine the mean detonation velocity (7337 m s^{-1}), whereas the OAM with bare optical probes (BOP) was used to measure the induced shock velocities generated by Seismoplast on different thicknesses of PMMA (1–9 mm), aluminum and copper (1–7 mm). Based on the shock velocities at the interfaces between the explosive and the inert barriers, the CJ pressure of Seismoplast was determined as 21.2 GPa.

Keywords: optical active method (OAM) · detonation pressure · shock wave velocity · impedance matching technique (IMT) · PETN based explosive

1 Introduction

The detonation wave (DW) structure, according to the Zeldovich–von Neumann–Döring (ZND) model, is composed by the von Neumann or chemical spike, which corresponds to a shock front followed by a chemical reaction zone; the Chapman-Jouguet (CJ) plane; and the Taylor wave that defines the isentropic expansion of the detonation products [1,2].

In the first half of the previous century, dynamic methods based on different physical principles, to determine detonation wave parameters, were developed worldwide [3]. Despite DW velocity being a relatively easy measurement, the detonation pressure (or CJ pressure) was, and still is, one of the most relevant parameters of biggest relevance [4]. However, authors of [5] believe that the experimental determination of this parameter is not widespread and computational calculations are preferred over the experimental tests.

The experimental methods that make it possible to determine the DW parameters are divided into two major groups: the internal and external methods [3,4]. Internal methods permit the direct measurement of the DW parameters, such as the particle velocities (u_p) of the detonation products inside the explosive charge and the direct determination of CJ pressure (P_{CJ}). The former parameter and, consequently, the P_{CJ} can be measured by the electromagnetic induction method [2,5] and the X-ray method [6]. The CJ pressure can be measured directly through the insertion of manganin [2,3,5,7] and/or polyvinylidene fluoride (PVDF) [3,8] pressure gauges into the sample of the explosive.

The external methods can be divided into three groups, defined by their measuring parameter: 1) measurement of the free surface velocities of an inert material (normally, a metallic foil); 2) determination of the velocity of the shock wave (SW) in a condensed inert material in contact with the explosive; and 3) direct determination of the induced pressure profile in an inert material. For 1), techniques such as electrostatic measurements of the SW velocity in PMMA barriers [2]; an array of electric pins connected to an oscilloscope [9]; using a streak camera to record argon-filled gaps [10], or the smear camera technique [11]; laser interferometric techniques [2], like Fabry-Perot [12], VISAR [13] and photonic Doppler velocimetry (PDV) [5,14,15] are used. Group 2) comprises methods such as streak cameras that can register images of a SW in water (aquarium test) [16], a moving copper grid in PMMA [9], or they can be connected

[a] J. Quaresma, L. Deimling
Fraunhofer-Institut für Chemische Technologie (ICT)
Joseph-von-Fraunhofer-Straße 7,
76327 Pfinztal, Germany
*e-mail: joana.quaresma@ict.fraunhofer.de
[b] J. Quaresma, J. Campos, R. Mendes
University of Coimbra, LEDAP, ADAI
Department of Mechanical Engineering
Rua Luís Reis Santos, Polo II, Coimbra,
3030-788 Coimbra, Portugal

© 2021 The Authors. Propellants, Explosives, Pyrotechnics published by Wiley-VCH GmbH. This is an open access article under the terms of the Creative Commons Attribution License, which permits use, distribution and reproduction in any medium, provided the original work is properly cited.

to optical fibers that are embedded in a PMMA barrier [17]; the short circuit of composite carbon-resistors embedded in a PMMA slab [18]; recording of the pulse voltages, originated by the detonation electric effect [19], with oscilloscopes; and the photoelectric method [20], where an inert liquid emits radiation proportionally to the pressure that it is being applied to it. In group 3), the induced pressure history is measured by manganin gauges embedded in thin Teflon barriers and the CJ pressure of the explosive calculated by the impedance matching technique. [7,17] The majority of these methods make it possible to determine the pressure at one point. However, determining the pressure field history *P*(t) over a charge diameter is possible by recording the detonation wave breakout through a Kapton stack monitor with argon-filled gaps on a streak camera [21,22,23], or by a line imaging velocity interferometer [24].

The explosive used in this work was Seismoplast, a PETN (86 %) based explosive normally used for civil purposes. In [18] was measured the CJ pressure of Seismoplast with composite carbon resistors. This method consists of putting two composite carbon resistors, which work as pressure transducers, into a polymethylmethacrylate (PMMA) slab. The pressures that these resistors can measure are a function of the nominal value of their resistance. These resistors are connected to a simple half-bridge circuit and their voltages are registered with an oscilloscope. The pressures are calculated, point by point, using calibration polynomials from SW experiments in water.

A device used to determine the detonation pressure based on the measurement of the SW propagation in inert materials with optical fibers, called OPTIMEX is described thoroughly in [25]. This technique is based on the measurement of the SW velocity, generated by the explosive A-IX-1 (95 % RDX), on four inert materials (Al, PMMA, PA6, and PTFE). The detonation pressure was determined by the impedance matching technique. The procedure used consisted in inserting 8 glass optical fibers (1 mm diameter) in the holes drilled in the inert material, all of them at different and well-defined depths. To generate a light pulse from the ionization of the air under the influence of the SW, an air cavity between the end of the hole and the tip of the fiber was created. The arrival times of the shock wave were read from the light traces and plotted against the corresponding distances. A quadratic equation was fitted to the data sets and the initial shock velocities in inert materials at $t = 0$ s were found as the first derivatives of the fitted equation at $t = 0$ *s*.

Since Seismoplast was used in this study, comprehensive literature research about the detonation characteristics of Seismoplast and PETN-based explosives was carried out. Seismoplast has few studies reporting its experimental detonation characteristics, such as the detonation velocity and CJ pressure. Table 1 shows such values according to the explosive density and charge geometry. The study [18] that was found about the experimental determination of Seismoplast's CJ pressure presents values that seem to be under-evaluated for a PETN based composition. Since Seismoplast is a PETN based explosive, it was necessary to search the literature about the CJ pressures of PETN based explosives to evaluate which pressure range would be reasonable for the CJ pressure of Seismoplast. Table 2 shows these CJ pressures for PETN based explosives in different forms and compositions. It also includes the references used from the literature review, the sample's density, detonation velocity, and the technique used to determine the pressure. The "different techniques" in Table 2 include laser measurement of wave velocity, velocity electrostatic measurements of shock waves in PMMA barriers, and the indicator fluid method.

This work encompasses a methodological description of the use of the optical active method (OAM) [29] for the measurement of the shock velocities (U_S), generated by an explosive on three different inert materials-PMMA, aluminum (Al), and copper (Cu) – to determine the CJ pressure of the explosive. A mathematical approach based on the movement of the SW, according to time, through different thicknesses of an inert material (*x(t)*) was used to determine the shock velocity of the inert material/explosive interface ($U_S(l)$) that corresponds to the CJ state, which characterizes the steady-state of the detonation. Calculations with two thermochemical equilibrium detonation codes, THOR and Explo 5, were made to predict the CJ pressure of the Seismoplast.

Table 1. Densities, charge's dimensions, detonation velocities, and CJ pressures of Seismoplast according to the respective experimental techniques.

ρ_0 ($g\,cm^{-3}$)	*Ch. dim.* (mm)	*D* ($m\,s^{-1}$)	P_{CJ} (GPa)	*Technique*
1.52	NR	7100	14.5	X-ray absorption*
1.52	h = 30, d = 36	7277	16	Carbon resistors [18]
NR	1.5 × 1.5 3 × 3 l = 52.5	6830–7800	NR	Rotating mirror streak and framing camera [26]
1.54	NR	7300	NR	NR [27]
1.56	h = 400, d = 50	7380	NR	Ionization pins (unpub.)

* work not available. Value referred at [18] NR – Not reported; h – height; d – diameter; l – length; unpub. – Fraunhofer ICT unpublished work.

 © 2021 The Authors. Propellants, Explosives, Pyrotechnics published by Wiley-VCH GmbH

Table 2. Densities, detonation velocity and CJ pressure values of PETN and respective experimental technique.

PETN form	ρ_0 (g cm^{-3})	D (m s^{-1})	P_{CJ} (GPa)	*Technique*
Crystalline	1.66	7950	27.0	Different techniques*
	1.76	8260	30.8	
Desensitized	1.66	8120	24.0	
NR	1.703	8100	28.0	
LX-16 (96.5% w/w)	1.734	8162	27.91	Photonic Doppler Velocity [4]
LX-16 (96.5% w/w)	1.734	8162	30.7	
LX-16 (96.5% w/w)	1.734	8153	30.0	Photonic Doppler Velocity [15]
Pressed charge	1.538	7675	22.47	High-speed photography.
Pressed charge	1.568	7794	23.99	IM: Water [16]
Pressed charge	1.46	7220	19.8	Shock electric effect [28]
(99% w/w)	1.53	7490	22.5	
	1.59	7710	25.9	

IM – Inert material; * works not available. Values referred at [2].

2 Experimental Section

2.1 Explosive

This work was performed with Seismoplast, a plastic, water-resistant, cap-sensitive explosive, based on PETN (85–86%) and an inert binder, with a density of 1.562 g cm^{-3}, that was produced by Orica (Germany) for seismic exploration [18, 26, 27, 28, 30].

2.2 Inert Materials

The Hugoniot constants (C_0, s) and densities (ρ_0) of the inert materials used in this work are presented in Table 3, as well as the respective bibliographic reference.

2.3 Optical System and Probe

The optical measurement system and probes used are fully described in [29].

The optical active method (OAM) is based on PMMA multimode optical probes that transmit laser radiation with a wavelength of 660 nm and stop the transmission when the probes are subjected to a shock wave. After passing through the probe, and before the radiation is converted into a voltage signal, it passes through a window filter with a bandwidth of between 650 and 670 nm to cut all undesirable radiation. Two kinds of probes were used: bare (BOPs) and protected (POPs) optical probes. The BOPs were used to measure the shock velocities and they were in direct contact with the explosive and/or with the inert material. The POPs were protected by stainless steel tubes and were used to measure the detonation velocity.

Table 3. ρ_0, C_0, and s parameters for each inert material used.

Inert material	ρ_0 (g cm^{-3})	C_0 (m s^{-1})	s (-)	Ref.
PMMA	1.186	2598	1.516	[5]
Al (1100)	2.714	5392	1.341	[31]
Cu	8.930	3940	1.489	[31, 32]

2.4 Experimental Set-Ups

The experimental set-ups used throughout this work are shown in Figure 1. The explosive charges were encased in PVC tubes with 150 mm length, 15.8 mm inner diameter, and 2.5 mm wall thickness. Six 0.5 mm diameter holes, spaced at 10 mm were then drilled up their height, to insert POPs. The detonation velocity of Seismoplast was determined for all the tests, with 2 or 6 POPs (Figure 1). To measure the SW propagation in inert materials, two barrier configurations were used: 1) the stacks barrier (Figure 1 upper) and 2) the single barrier (Figure 1, lower). Configuration 1 had a PMMA block to support the PVC tube followed by the PMMA's stack of barriers, which were composed of three consecutive 1 mm thick plates, followed by two 2 mm thick plates, and support plate. All the PMMA plates were squares of 50 mm on all sides; each square had one slit (0.3 mm deep) on its upper face to accommodate BOPs; the BOPs slits were open at a distance of 4 mm from the center of the charge and the plates with the slits were arranged to space the slits equally between them, avoiding their superposition, as represented on the top right-hand side of Figure 1. All the experiments had an aluminum plate to support the whole set-up. Only one squared PMMA plate was used (100×100 mm), its thickness varied between 0.5 and 10 mm, and the two probes were crossed at the axis of the cylindrical charge, in configuration 2 (Figure 1, bottom).

 © 2021 The Authors. Propellants, Explosives, Pyrotechnics published by Wiley-VCH GmbH

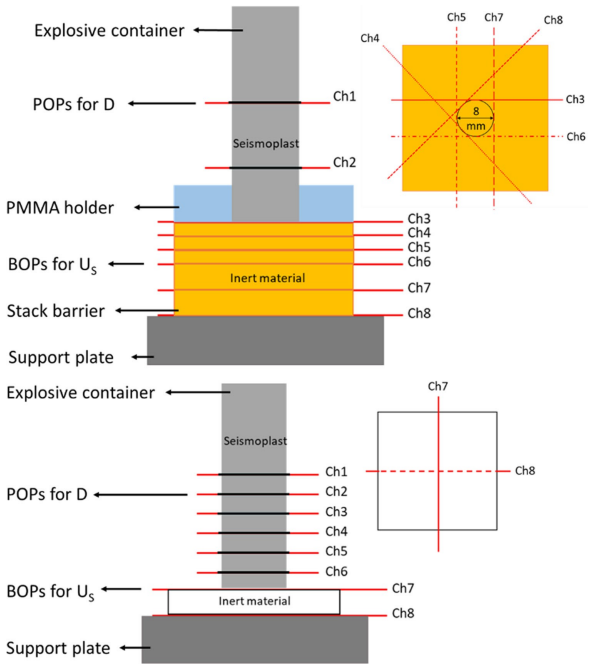

Figure 1. The configurations set-up to measure the shock velocity on inert stack barrier of PMMA, Al, and Cu (top) and a single plate (bottom).

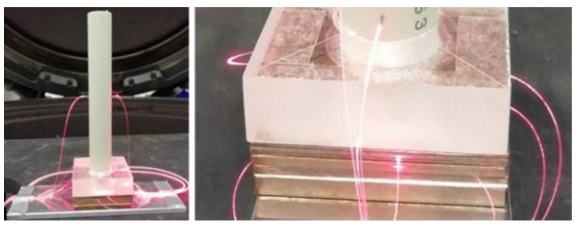

Figure 2. Complete sample assembly (left) and zoomed image (right) of a configuration 1 prepared to characterize the shock wave velocity in Cu. The PMMA block, above the Cu stack, worked as a charge holder. The active optical probes are conducting the red laser radiation.

Some experiments had slits to accommodate the probes, while others did not.

All the set-ups were prepared in the lab, only the Seismoplast was loaded manually into the container immediately before the experiment, with tools specially designed for this propose.

Configuration 1 was used for PMMA, Al, and Cu, while configuration 2 was only used for PMMA. Figure 2 shows a configuration 1 prepared to characterize the shock wave propagation in a Cu barrier.

3 Results and Discussion

The numerical calculations for the detonation velocity and CJ pressure of the Seismoplast, as well as a description of the experimental data recorded, the analysis of the shock velocity in inert barriers in terms of *x(t)* plot, and the mathematical procedures for the determination of CJ pressure, will be presented in this section.

3.1 Theoretical Predictions

Due to the lack of literature concerning Seismoplast (Table 1) and to complement the literature review for experimental data about PETN based explosives (Table 2), theoretical calculations about Seismoplast CJ pressure were made and used as reference values for comparison with the ones obtained experimentally in this work. These theoretical predictions were made resorting to two different thermochemical equilibrium detonation codes, THOR [33] and Explo 5 [34].

Table 4 presents the CJ pressures for Seismoplast determined with THOR and Explo 5 codes. Table 4 also shows the densities used in each calculation and the detonation and particle velocities predicted at the CJ point. These calculations were done for 86% PETN and 14% Sylgard (silicone resin) as the reactants. The actual composition of Seismoplast, according to [18] includes 13% of Sylgard and 1% of zinc stearate. Since the second compound is not present in THOR's database, it was substituted by Sylgard because both of them are components of the inert binder. Both codes used the BKW equation of state (EoS), except for the THOR* calculation. This was done using HL EoS [35], because this EoS is optimized on THOR [33], to work with condensed products of the reaction.

The computational data for P_{CJ} presented in Table 4 are higher than the ones for Seismoplast presented in Table 1. The experimental CJ pressure of Seismoplast in [18] seems under-evaluated for an explosive with 86% of PETN (Table 1) because, according to the literature about explosives with PETN compositions with a density and a detonation velocity similar to Seismoplast (Table 2), it is expected that the CJ pressure of such explosive composition varies between 19.8 and 23.99 GPa [28, 16].

Table 4. ρ_0, D, $u_{P,CJ}$, and P_{CJ} of Seismoplast according to the theoretical predictions.

Code	ρ_0 (g cm^{-3})	D_{CJ} (m s^{-1})	$u_{P,CJ}$ (m s^{-1})	P_{CJ} (GPa)
Explo 5	1.56	7219	1958	22.1
THOR	1.56	7670	1746	20.8
THOR*	1.56	7669	1761	21.0

* HL EoS

© 2021 The Authors. Propellants, Explosives, Pyrotechnics published by Wiley-VCH GmbH

The computational results are shown in Table 4, which present a CJ pressure range from 20.8 to 22.1 GPa for a density of 1.56 g cm^{-3}, are more in agreement with the experimental data available for PETN based explosives (Table 2) with similar detonation velocity and density to Seismoplast.

3.2 Signal Interpretation

The signals obtained during this study for measuring the detonation and shock velocities were acquired using the OAM, whose principle is summarized at 2.3 and analyzed and described in more detail in [29].

Figure 3 displays the electrical signals generated by POPs and BOPs using the OAM, when this optical method is applied to measure the detonation pressure, according to the setup depicted in Figure 1. Channels Ch1 and Ch2 correspond to the passage of the DW through POPs 1 and 2. Channel Ch3 corresponds to the BOP inserted in the interface explosive/PMMA and channels Ch4 to Ch8 correspond to the BOPs that are between the PMMA plates. These signals obey the description made in 2.3. The electrical signals generated by the BOP's inside the Al or Cu barriers are similar to the ones obtained from the PMMA's stack of barriers and showed in Figure 3.

The abrupt break in the shape of the optoelectric signals obtained was used to identify the arrival time of the DW/SW to the probe and it was similar for all set-ups, independently of the inert material's nature (opaque, translucent, or porous) and independently of the radiation generated by the DW or by the compressed air gap, as opposed to what happed in [25], where it is stated that the shape of the optoelectric signal is dependent of the inert barrier used and the SW's ability to ionize the air in the cavity where the probe is inserted. In all the materials used (transparent and opaque), the optical active method using BOPs made it possible to identify the time instant when the probes were hit by the SW clearly without any constraints originating from the production of light

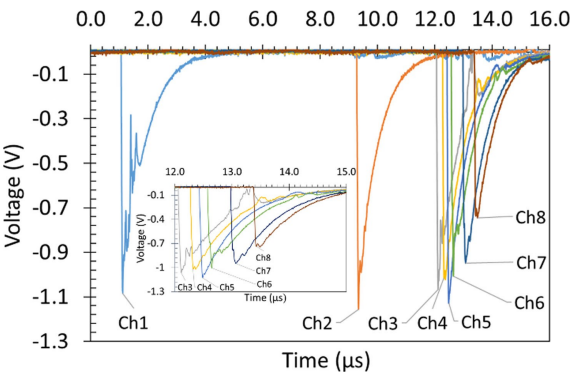

Figure 3. Electrical signals obtained for detonation velocity calculation (Ch1 and Ch2) and shock velocity calculation (from Ch3 to Ch8) in the PMMA stack monitor.

during the measurements. The time measurements were made according to [29].

3.3 Detonation Velocity

Depending on the set-up used, 2 or 6 velocity probes were used for an explosive column length of 50 mm to determine the detonation velocity (D). The D determined and used throughout this work was 7337 ± 52 m s^{-1} (associated relative error of 0.7 %), and it was calculated according to equation (1), where D_i is the interval velocity value between two consecutive probes, calculated for each space (Δx_i) and time interval (Δt_i).

$$D_i = \frac{\Delta x_i}{\Delta t_i} \quad i = 0, \ldots, 5 \tag{1}$$

The displacement (Δx_i) corresponds to the distances between two consecutive probes and has a systematic error of ± 0.05 mm associated with the CNC machines used to open the slits. The time intervals (Δt_i) corresponds to the time difference between two consecutive probes, and have a systematic error of ± 4.2 ns, which is related to the temporal resolution of the transient recorder, and i corresponds to the interval analyzed. The recording of the times from the electric signals and the procedure to determine the detonation velocity (D) are described comprehensively in [29].

3.4 Detonation Pressure

The detonation pressure determination that will be presented is based on the impedance matching technique (IMT), performed to obtain the CJ pressure of Seismoplast by registering the movement of the SW along with the inert material according to time ($x(t)$ plot), and the determination of the shock velocity of the Seismoplast/inert material interface ($U_S(I)$).

3.4.1 Determination of the Explosive-Inert Material Interface State

The Ch3 to Ch8 signals shown in Figure 3 make it possible to identify the time that the SW needs to reach each optical probe installed in the inert barriers and, consequently, to determine the (x, t) diagram for the SW movement. Figure 4 shows the movement of the SW generated by Seismoplast, through different thicknesses of PMMA, Al, and Cu, according to time.

The experimental points representing the propagation of SW in inert materials were fitted with a quadratic trend line to obtain the quadratic $x(t)$ function that described the movement of the SW in the inert material. These fitting equations ($x(t)$) are shown in Table 5.

 © 2021 The Authors. Propellants, Explosives, Pyrotechnics published by Wiley-VCH GmbH

Table 5. Parameters calculated for PMMA, Al and Cu.

Parameter	*PMMA*	*Al*	*Cu*
$x(t)$ [mm]	$-0.638\ t^2 + 6.072\ t + 0.076$	$-0.648\ t^2 + 7.242\ t + 0.405$	$-0.849\ t^2 + 5.118t - 0.03$
R^2	0.993	0.983	0.998
$U_S(I)$ [m s^{-1}]	6072	7242	5118
$u_P(I)$ [m s^{-1}]	2292	1380	791
$P(I)$ [GPa]	16.5	27.1	36.2

The shock velocity in the Seismoplast/inert material interface ($U_S(I)$) was obtained from the first derivative of $x(t)$ of each material, for t = 0 s, and they are displayed in Table 5.

After finding the interface shock velocity $U_{S,IM} = U_S(I)$, and using the C_0 and s values presented in Table 3, it was possible to calculate the particle velocity at the interface $u_{P,IM} = u_P(I)$ and the pressure $P_{IM} = P(I)$ at the Seismoplast/inert material interface according to eq. (2) and eq. (3) respectively, where the subscript *IM* means inert material.

$$U_{S,IM} = C_{0,IM} + s_{IM} u_{P,IM} \tag{2}$$

$$P_{IM} = \rho_{0,IM} U_{S,IM} u_{P,IM} \tag{3}$$

The calculated results ($u_P(I)$ and $P(I)$) for each inert material are presented in Table 5.

Considering that the loading off-axis is not 1D along the path of interest in configuration 1, some of the latter probes inserted in the inert material, suffer attenuation from the lateral release of the SW. The extension of this phenomenon depends on the ratio between the axial shock velocity and the velocity of the lateral release. This phenomenon will affect the shock velocity and the CJ pressure in a similar way as demonstrated by Bourne [36]. The errors caused by these phenomena will be evaluated in further investigations.

3.4.2 Impedance Matching Technique

Once the interface shock velocities for each inert material, as well as their respective interface pressures ($P(I)$) and particle velocities ($u_P(I)$), were obtained, it was possible to represent them graphically on the Hugoniot of each material (PMMA, Al and Cu), as it is shown on Figure 5.

Figure 5 shows the Hugoniot for each inert material, the R line, and the quadratic fitting made to the interface points. It also represents the interface state of each material after being shocked by Seismoplast, as well as the respective CJ point.

The CJ pressure was obtained as an intersection of a quadratic fit through the three interface states and the Rayleigh line. This fitting included the states above the CJ state, which are on the Hugoniot of the detonation products, as well as the states below CJ that are located at the isentropic of the detonation products. The intersection of this fitting with the Rayleigh line provided the P_{CJ}.

The CJ pressure obtained by this method was 21.2 GPa, which is very close to the results of the computational calculations.

3.5 Discussion of Results

The experimental value of the detonation pressure of Seismoplast calculated in this work was 21.2 GPa. This value is

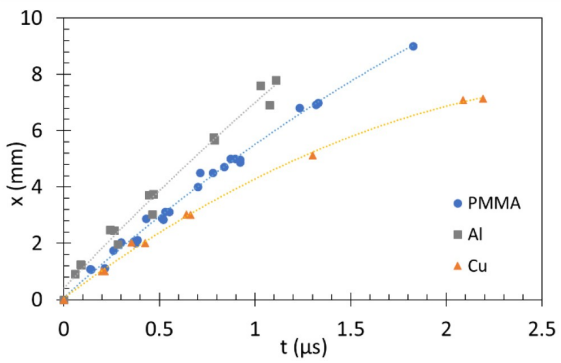

Figure 4. $x(t)$ diagrams of the shock waves generated through different thicknesses of the inert materials by Seismoplast.

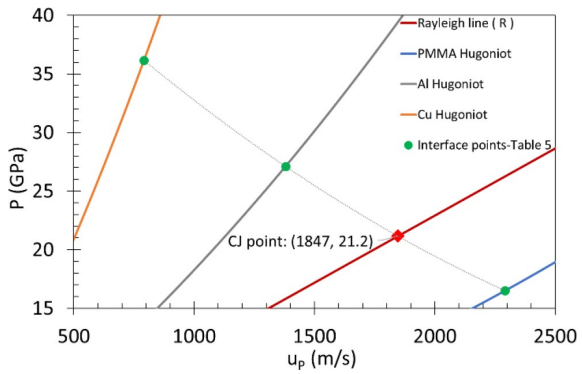

Figure 5. Determination of the CJ point of Seismoplast by fitting to the interface Seismoplast/inert material characteristic points ($P(I)$ and $u_P(I)$ values from Table 5).

 © 2021 The Authors. Propellants, Explosives, Pyrotechnics published by Wiley-VCH GmbH

significantly higher than the ones presented in Table 1. However, it is in line with the detonation pressures for the PETN based compositions presented in Table 2, for compositions that have similar densities or similar detonation velocities.

Further, the values obtained are in agreement with the computational calculations performed with different EoS and codes for Seismoplast with a density of 1.56 g/cm^3, which presents a detonation pressure range from 20.8 to 22.1 GPa. The CJ pressures determined with the BKW EoS, in both thermochemical equilibrium codes, exhibit a difference of 1.3 GPa. Among the possible reasons, one is related with the different values for the BKW constants (α, β, κ, θ) used in both codes. EXPLO5 considers the BKWN EoS with (0.5, 0.38, 9.4, 4120), while THOR uses the BKW EoS with (0.5, β, 11.8, 400). The constant β is determined according to the richness of the mixture, varying between 0.16 (β for RDX, richness = 1.5) and 0.096 (β for TNT, richness = 2.75). Another reason may be related to the amount of solid carbon in the detonation products, which is almost double in THOR than is in EXPLO5, whereas the amount of SiO_2 (s) is similar in both codes.

As previously mentioned, the SW arrival time to some of the latter probes was affected by the lateral release, in configuration 1. In future work, the errors revealed in these probes that slightly affect the $U_S(I)$, and consequently the value of the CJ pressure, will be clarified.

4 Conclusions

The optical active method (OAM) was applied to determine the detonation pressure of Seismoplast, a PETN based explosive. The experimental method was based on the analysis of the SW propagation in inert barriers, which were PMMA, Al, and Cu. Two different set-ups were used to measure the SW velocity: a single barrier and a stack of barriers.

According to the *x(t)* plot, the CJ pressure obtained by the quadratic fitting was 21.2 GPa for Seismoplast with a density of 1.56 g cm^{-3}.

All the measurement data shown in this work are in agreement with the calculations performed using the thermochemical equilibrium codes.

Symbols and Abbreviations

PETN	Pentaerythritol tetranitrate or penthrite
PBX	Plastic-bonded explosive
OAM	Optical active method
PMMA	Poly(methyl methacrylate)
DW	Detonation wave
SW	Shock wave
POP	Protected optical probe
BOP	Bare optical probe
IMT	Impedance matching technique
ZND	Zeldovich–Neumann–Döring
CJ	Chapman-Jouguet
u_P	Particle velocity
PVDF	Polyvinylidene fluoride
PDV	Photonic Doppler velocimetry
RDX	Cyclotrimethylenetrinitramine
Al	Aluminium
PA6	Polycaprolactam
PTFE	Polytetrafluoroethylene
U_S	Shock velocity
Cu	Copper
x(t)	Position of the SW according to time
D	Detonation velocity
P_{CJ}	Chapman-Jouguet pressure
ρ_0	Initial density
IM	Inert material
FPLI	Fabry-Perot Laser Interferometer
LiF	Lithium fluoride
EoS	Equation of state
C_0	Bulk sound velocity
s	Constant
D_i	Interval detonation velocity value
Δx_i	Distance
Δt_i	Time interval

Acknowledgement

Open access funding enabled and organized by Projekt DEAL.

Data Availability Statement

No Data available.

References

[1] R. E. Duff, E. Houston, Measurement of the Chapman-Jouguet Pressure and Reaction Zone Length in a Detonating High Explosive, *J. Chem. Phys.* **1955**, *23*, 1268. https://doi.org/10.1063/1.1742255.

[2] L. Al'tshuler, G. Doronin, V. Zhuchenko, Detonation regimes and Jouguet parameters of condensed explosives, *Combust. Explos. Shock Waves* **1989**, *25*, 209. Doi: 10.1007/BF00742019.

[3] M. Suceska, *Test Methods for Explosives*, Springer-Veria, New York **1995**.

[4] M. Chaos, E. L. Lee, K. T. Lorenz, Experimental Determination of Chapman-Jouguet Pressure Using Disc Acceleration eXperiment (DAX) Data, *16th International Detonation Symposium*, July 15–20, **2018**, Cambridge, MD, United States. https://www.osti.gov/servlets/purl/1465298.

[5] J. Pachman, M. Künzel, O. Ňemec, J. Majzlík, A comparison of methods for detonation pressure, *Shock Waves* **2018**, *28*, 217. https://doi.org/10.1007/s00193-017-0761–5.

[6] W. C. Rivard, D. Venable, W. Fickett, C. Davis, Flash x-ray obseervation of marked mass points in explosive products, *Fifth Symposium (international) on Detonation*, August 18–21, **1970**, Pasadena, California, USA.

 © 2021 The Authors. Propellants, Explosives, Pyrotechnics published by Wiley-VCH GmbH

[7] R. Mendes, J. Ribeiro, I. Plaksin, J. Campos, B. Tavares, Differences between the detonation behavior of emulsion explosives sensitized with glass or with polymeric micro-balloons, *J. Phys. Conf. Ser.* **2014**, *500*, 052030. doi:10.1088/1742-6596/500/5/052030.
[8] L. M. Lee, R. A. Graham, F. Bauer, R. P. Reed, Standartized Bauer PVDF Piezoelectric polymer shock gauge, *Le Journal de Physique Colloques* **1988**, *9*. doi: 10.1051/jphyscol:1988391.
[9] M. Held, Determination of the Chapman- Jouguet Pressure of a High Explosive from One Single Test, *Def. Sci. J.* **1987**, *37*, 1. doi: 10.1002/1521-4087(200203)27:13.0.CO;2-A.
[10] I. Plaksin, J. Campos, J. Ribeiro, R. Mendes, J. Gois, A. Portugal, P. Simoes, L. Pedroso, Detonation meso-scale tests for energetic materials, *AIP Conf. Proc.* **2002**, *620*, 922. https://doi.org/10.1063/1.1483688.
[11] W. C. Davis, B. G. Craig, Smear Camera Technique for Free-Surface Velocity Measurement, *Rev. Sci. Instrum.* **1961**, *32*, 579. https://doi.org/10.1063/1.1717443.
[12] A. V. Fedorov, A. L. Mikhailov, L. K. Antonyuk, D. V. Nazarov, S. A. Finyushin, Determination of Parameters of Detonation Waves in PETN and HMX Single Crystals, Combustion, *Explosion, and Shock Waves* **2011**, *47*, 601. doi:10.1134/S0010508211050145.
[13] V. Bouyer, M. Doucet, L. Decaris, Experimental measurements of the detonation wave profile in a TATB based explosive, *EPJ Web of Conferences* **2010**, *10*, 00030. doi:10.1051/epjconf/20101000030.
[14] J. Pachman, M. Künzel, O. Němec, S. Bland, Characterization of Al Plate Acceleration by Low Power Photonic Doppler Velocimetry (PDV), *40th International Pyrotechnics Society Seminar*, July 13–18, **2014**, Colorado Springs, Colorado USA.
[15] K. T. Lorenz, E. L. Lee, R. Chambers, A Simple and Rapid Evaluation of Explosive Performance–The Disc Acceleration Experiment, *Propellants Explos. Pyrotech.* **2015**, *40*, 95. doi:10.1002/prep.201400081.
[16] N. L. Coleburn, Chapman-Jouguet pressures of several pure and mixed explosives, United States Naval Ordnance Laboratory, White Oax, Maryland, USA, **1964**. https://apps.dtic.mil/dtic/tr/fulltext/u2/603540.pdf.
[17] R. Mendes, J. Ribeiro, I. Plaksin, J. Campos, Non ideal detonation of emulsion explosives mixed with metal particles, *AIP Conf. Proc.* **2012**, *1426*, 267. doi:10.1063/1.3686270.
[18] K. Hollenberg, Time Resolved Pressure Measurement of the Initiation in Gap Test Experiments, *Propellants Explos. Pyrotech.* **1986**, *11*, 155. doi:10.1002/prep.19860110506.
[19] B. Hayes, The Detonation Electric Effect, *J. Appl. Phys.* **1967**, *38*, 507. https://doi.org/10.1063/1.1709365.
[20] B. G. Loboiko, S. N. Lubyatinsky, Reaction Zones of Detonating Solid Explosives, *Combust. Explos. Shock Waves* **2000**, *36*, 716. https://doi.org/10.1023/A:1002898505288.
[21] I. Plaksin, J. Direito, J. Campos, J. Ribeiro, R. Mendes, C. Cofey, J. Kennedy, Meso-scale probing of CRZ structure in PBX: DW oscillations from ignition to failure, *AIP Conf. Proc.* **2006**, *845*, 1002. doi:10.1063/1.2263491.
[22] I. Plaksin, L. Rodrigues, S. Plaksin, J. Campos, R. Mendes, J. Ribeiro, J. Gois, Radiation-induced percursors in crystalline energetic composites, *AIP Conf. Proc.* **2009**, *1195*, 137. doi:10.1063/1.3295066.
[23] I. Plaksin, L. Rodrigues, S. Plaksin, J. Campos, R. Mendes, J. Ribeiro, Effect of the Reaction Light Absorption on the Formation of the Detonation Reaction Zone 3D-Structure, *14th International Detonation Symposium*, IDS **2010**, 241.
[24] P. M. Celliers, D. K. Bradley, G. W. Collins, D. G. Hicks, T. R. Boehly, W. J. Armstrong, Line-imaging velocimeter for shock diagnostics at the OMEGA laser facility, *Rev. Sci. Instrum.* **2004**, *75*, 4916. https://doi.org/10.1063/1.1807008.
[25] M. Künzel, A. C. Anastacio, J. Kucera, J. Pachman, OPTIMEX: Detonation pressure determination using passive optical system, *Proceedings of the 20th Seminar on New Trends in Research of Energetic Materials*, April 26–28, **2017**, Pardubice, Czech Republic, 726–730.
[26] M. Held, Initiation Tests, *Propellants Explos. Pyrotech.* **2002**, *27*, 39. https://doi.org/10.1002/1521-4087(200203)27:1<39::AID-PREP39>3.0.CO;2-A.
[27] J. Köhler, R. Meyer, Explosivstoffe, 10 ed., Wiley-VCH, Weinheim **2008**.
[28] H. C. Hornig, E. L. Lee, M. Finger, J. E. Kurrle, Equation of State of Detonation Products, *Fifth Symposium (international) on Detonation*, August 18–21, **1970**, Pasadena, California, USA.
[29] J. Quaresma, L. Deimling, J. Campos, R. Mendes, Active and Passive Optical Fiber Metrology for Detonation Velocity Measurements, *Propellants Explos. Pyrotech.* **2020**, *45*, 921. doi:10.1002/prep.201900197.
[30] S. Thiboutot, P. Brousseau, G. Ampleman, Deposition of PETN Following the Detonation of Seismoplast Plastic Explosive, *Propellants Explos. Pyrotech.* **2015**, *40*, 329. doi:10.1002/prep.201500019.
[31] S. P. Marsh, *LASL Shock Hugoniot Data*, University of California Press, Los Alamos **1980**.
[32] L. Davison, *Fundamentals of Shock Wave Propagation in Solids*, Springer, Berlin **2008**.
[33] J. Campos, R. Mendes, and J. Quaresma, Prediction of deflagration and detonation products properties, using THOR code procedures and parameters, *49th International Annual Conference of the Fraunhofer ICT*, June 26–29, **2018**, Karlsruhe, Germany, 7/1–7/12.
[34] M. Suceska, Evaluation of Detonation Energy from EXPLO5 Computer Code Results, *Propellants Explos. Pyrotech.* **1999**, *24*, 280. https://doi.org/10.1002/(SICI)1521-4087(199910)24:5<280::AID-PREP280>3.0.CO;2-W.
[35] L. Durães, J. Campos, J. C. Gois, New Equation of State for the Detonation Products of Explosives, *AIP Conf. Proc.* **1996**, *370*, 385. https://doi.org/10.1063/1.50802.
[36] N. K. Bourne, G. A. Cooper, S. J. Burley, V. Fung, R. Hollands, Re-Calibration of the UK Large Scale Gap Test, *Propellants Explos. Pyrotech.* **2005**, *30*, 196. doi: 10.1002/prep.200500005.

Manuscript received: August 4, 2020
Revised manuscript received: January 29, 2021
Version of record online: March 30, 2021

 © 2021 The Authors. Propellants, Explosives, Pyrotechnics published by Wiley-VCH GmbH